Effect of the Surface Roughness and Construction Material on Wall Slip in the Flow of Concentrated Suspensions

Sergul Acikalin Gulmus, Ulku Yilmazer

Department of Chemical Engineering, Middle East Technical University, Ankara 06531, Turkey

Received 24 December 2005; accepted 6 September 2006
DOI 10.1002/app.25468
Published online in Wiley InterScience (www.interscience.wiley.com).

ABSTRACT: Recent studies on polyethylene, elastomers, and thermoplastics have revealed that the construction material and surface roughness are two important factors affecting wall slip. In this study, to determine the true rheological behavior of model concentrated suspensions, a multiple-gap separation method was used in a parallel disk rheometer. The model suspensions studied were poly (methyl methacrylate) particles with an average particle size of 121.2 μm in hydroxyl-terminated polybutadiene. The aim of this study was to investigate the effect of disk R_a in the range of 0.49–1.51 μm and disk construction material on the wall slip and the true viscosity of the model concentrated suspensions. The wall slip velocity and the viscosity were found to be independent of R_a for particle size-to-disk R_a ratios of 80–247. Also, the true viscosity was found not to be affected by the rheometer surface construction material. Glass surfaces resulted in the highest slip velocity, whereas aluminum surfaces resulted in the lowest slip velocity. © 2006 Wiley Periodicals, Inc. J Appl Polym Sci 103: 3341–3347, 2007

Key words: rheology; surfaces; shear; viscosity

INTRODUCTION

The rheological behavior of polymeric suspensions depends on the particle shape, size and size distribution; volume fraction of particles; particle–particle and particle–matrix interactions; matrix rheology and measurement conditions such as the temperature and shear rate. In addition, recent studies[1–16] on poly ethylene (PE), elastomers and thermoplastics have revealed that the construction material and surface roughness (R_a) are two important factors affecting wall slip. Grooved or roughened surfaces are often used during the rheological characterization of various materials to eliminate wall slip with different construction materials. Roughened rheometer surfaces are also used during the rheological characterization of materials such as gels, emulsions, and greases.

Vinogradov et al.[1] showed that the wall effect substantially influences the flow curves obtained with smooth capillaries, especially at low shear rates. The magnitude of this effect is estimated as a function of the capillary radius and shear rate at the capillary wall. It has been proven experimentally that the use of grooved surfaces eliminates the wall effect. The properties of the wall layer are assessed with the concept of the activation nature of the viscous flow of disperse systems. The thickness, disperse-phase concentration, and viscosity characteristics of the wall layer are determined from the variations of the free activation energy in the wall layer and in the bulk of the fluid. On the basis of the concept of the activation mechanism of the flow process, Vinogradov et al.[2] introduced characteristic parameters that have the dimension of length and that depend on the shape and the size of the measuring surfaces. The use of these parameters results in a linear relationship between the apparent rate of shear and the characteristic sizes of the measuring surfaces. Thus, it is possible to calculate the rate of the shear gradient for the system in the bulk and, hence, to find the true flow curves for plastic disperse systems.

The hydrodynamic resistance of adsorbed polymer layers to the flow of aqueous and organic polymer solutions in stainless steel capillary tubes was experimentally quantified with a surface treatment method by Cohen and Metzner.[3] They observed that for a given shear rate, the shear stress is higher for untreated tubes than for treated tubes. In other words, a higher apparent viscosity is observed in untreated tubes.

It is known that the adhesion at a melt–metal interface is influenced by both the roughness and the chemical nature of the surfaces. Kraynik and Schowalter[4] studied wall slip during the flow of viscoelastic fluids through cylindrical tubes and the surface character of the extrudate with aqueous solutions of poly(vinyl alcohol) and sodium borate. They

Correspondence to: U. Yilmazer (yilmazer@metu.edu.tr).

Journal of Applied Polymer Science, Vol. 103, 3341–3347 (2007)

showed that the microscopic nature of a tube wall could promote or inhibit slip and that slip reduced extrudate swell and delayed the onset of severe extrudate distortion.

Jiang et al.[5] also observed, with hydroxypropyl guar gels, that wall slip occurred more readily in tubes with smooth surfaces. The wall slip of gels was observed more readily in acrylic tubes, as compared to stainless steel tubes.

Ramamurthy[6] examined the question of slip and the influence of materials of construction on observed extrudate irregularities for high-viscosity molten PE. Contrary to capillary rheometer observations, blown-film fabrication results for linear low-density polyethylene (LLDPE) indicate that construction materials for the die land region had a significant influence on the melt fracture and suggested breakdown of adhesion at the polymer–metal interface as a primary cause of slip and melt fracture. The results demonstrate that methods for improving adhesion by the proper choice of construction materials for the die land region and/or the use of adhesion promoters in the resin virtually eliminated the rate-limiting effects of melt fracture in commercial blown-film fabrication.

Chen et al.[7] investigated the effects of construction materials and surface roughness on the wall slip behavior of a LLDPE with capillaries constructed from copper, stainless steel, aluminum, and glass. They observed that the wall slip velocity values increased with decreasing surface roughness of the capillaries and with decreasing work of adhesion. The relative slip behavior of PE in the various capillaries was related to the competing effects of surface roughness and the work of adhesion. The highest wall slip velocities were observed with stainless steel, which exhibited a relatively small work of adhesion and a capillary surface roughness transverse to the flow direction. The no-slip condition observed for aluminum was related to the porous nature and relatively higher roughness of the aluminum surface and the moderate adhesion of PE to aluminum.

The effects of surface topology and energy on the stick–slip transition were studied in the capillary flow of highly entangled PE melts by Wang and Drda.[8] Surface roughness was shown to increase the critical stress of the stick–slip transition because of the increased resistance to interfacial disentanglement. Lowering the surface energy of a smooth die wall by treatment with fluorocarbon completely eliminated the stick–slip transition. Additionally, a slip–slip transition was found in the die with a nearly nonadsorbing wall, which appeared to involve a secondary chain-debonding process.

Wang and Drda[9] also observed that depending on the surface condition of the die wall, two distinctly different molecular processes might have caused interfacial slip for the same PE resin. One form of slip occurred when a critical stress was reached; this depended on temperature. However, the magnitude of the stick–slip transition as given by an extrapolation length was independent of temperature. Another mechanism for interfacial slip appeared to originate from a lack of polymer adsorption at a low surface energy die wall and involved at least two sequential transitions, a transformation of the melt–wall boundary condition from no-slip to slip at rather low stresses due most likely to stress-induced desorption of adsorbed chains and a slip–slip transition occurring at a very high critical stress, presumably due to debonding of the few surviving adsorbed chains.

Yang and coworkers[10,11] conducted a comprehensive experimental study of the melt–wall interfacial slip behavior of various polymer melts in capillary flow. They observed that none of the six polymers they studied exhibited an interfacial stick–slip transition or showed any sign of wall slip in bare aluminum dies. However, they displayed a sizeable wall slip by lowering the die wall surface energy with a fluoropolymer coating. The degree of wall slip was characterized by extrapolation length, which was demonstrated to be explicitly proportional to the melt viscosity, such that the magnitudes of wall slip in the coated die decreased with increasing shear thinning.

Ghanta et al.[12] extruded LLDPE through capillary dies fabricated from stainless steel and brass. They confirmed results first reported by Ramamurthy[6] that sharkskin could be eliminated by the use of a brass die. They found a substantially enhanced throughput from the brass die relative to the stainless steel die at stresses in the range where sharkskin was observed with the latter.

Jabbarzadeh et al.[13] reported a molecular dynamics simulation of a thin liquid film as it was sheared between two planar walls. In their model, bond stretching, angle bonding, and dihedral potentials were included. Different properties of the wall, such as wall density, wall stiffness, and wall–fluid interaction strength were studied to determine the slip between the wall and fluid. Slip was investigated for strong and weak adsorbing surfaces at various shear rates. The results emphasize the importance of adsorption on the degree of slip. The dependence of slip on the film thickness was also demonstrated.

Barone and Wang[14] reiterated that the molecular mechanism for wall slip in polymer liquids could change from cohesive to adhesive failure at the polymer wall interface when the wall surface changes from inorganic materials to organic coatings. In particular, the spurt flow behavior, that is, the stick–slip transition observed at a critical applied stress in steel or aluminum dies arose from cohesive wall slip and was not due to polymer desorption. On the other hand, good organic coatings allowed adhesive wall slip to occur at significantly lower stresses.

In addition to the investigations about the true slip of polymer melts, the apparent slip of concentrated suspensions has been also reported in the literature, and in particular for highly concentrated suspensions, slip at the wall has been found to be a controlling factor. The difference between the apparent and true wall slip mechanism, respectively, for suspensions and polymer melts has also been mentioned in these studies. Although in the true slip mechanism of polymer melts, a discontinuity in the velocity between the polymer and the wall occurs, in the apparent slip mechanism of suspensions, a large velocity gradient occurs near the wall in the low-viscosity resin-rich layer.

Although several studies have been done on polymer melts and solutions, there is a lack of literature about the effects of surface roughness and construction material on the wall slip phenomenon of concentrated suspensions.

Kalyon et al.[15] used aluminum oxide and silicon carbide impregnated parallel disks and was successful in preventing wall slip of a concentrated suspension under some small-amplitude oscillatory shear conditions. Later, Aral and Kalyon[16] used disks with a wide range of R_a values and observed that the use of roughened disks prevented slip; however, generally, sample fractures were observed. Fracture effects were also observed to become dominant with increasing R_a values. Aral and Kalyon[16] studied particle size-to-R_a ratios of approximately 0.34 to 227.7 (assuming that their disk had a diameter of 12.5 mm). They observed slip roughly when the ratio was higher than 1 and no slip when this ratio was smaller than 1. Sample fracture was observed usually when slip did not occur. This ratio was between 80 and 247 in our study; thus, slip was observed for all of the cases studied.

The aim of this study was to investigate the effects of rheometer surface roughness and rheometer surface material on the wall slip of concentrated polymeric suspensions and to determine the true viscosity of these model concentrated polymeric suspensions. This was achieved by use of the multiple-gap separation technique[17,18] with a parallel disk rheometer. This information has been lacking in the literature.

EXPERIMENTAL

Materials

The polymer matrix of the concentrated suspensions studied was hydroxyl-terminated polybutadiene (HTPB; Atlantic Richfield, Los Angeles, CA). This polymer has a specific gravity of 0.786. In the shear rate range of 0.04–0.6 s^{-1}, the shear viscosity of HTPB was found to be 2.4 Pa s at 25°C, independent of the deformation rate.

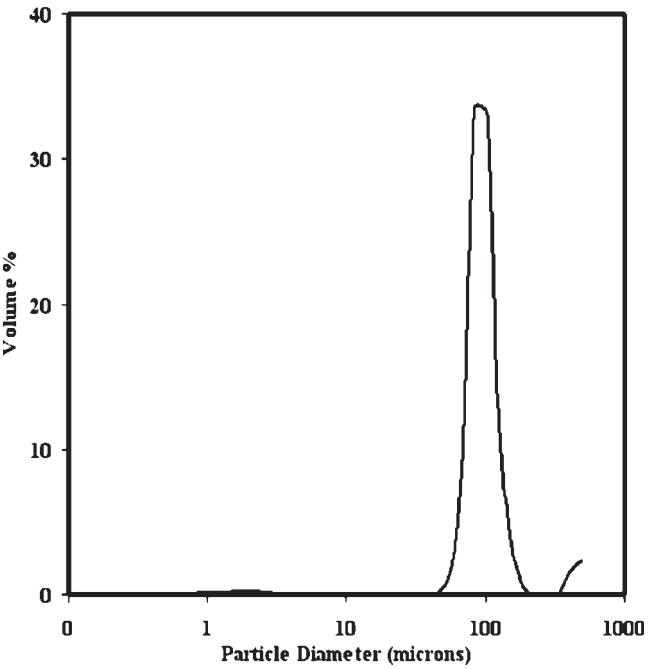

Figure 1 Particle size distribution of PMMA.

The suspensions were prepared with solid spherical particles of poly(methyl methacrylate) (PMMA; Meliodent, Bayer Dental, Leverkusen, Germany). The size distribution of the particles, determined by Mastersizer X from Malvern Instruments (Malvern, UK), is shown in Figure 1. The average particle size of the PMMA particles was 121.2 μm, and their specific gravity at 25°C was 1.19.

Preparation of the suspension samples

In the material preparation, the first step was to determine the maximum packing fraction of PMMA. The maximum packing fraction determination was done by the sedimentation in air method. Particles were poured into a container by vibration, and the container was tapped at certain time intervals. Then, the maximum volume packing fraction (ϕ_m) was determined as 0.646 by eq. (1):

$$\phi_m = \phi_{app}/\phi_{ac} \quad (1)$$

where ϕ_{app} and ϕ_{ac}, are the apparent and actual densities, respectively, of the particles.

In the second step, the mixing of HTPB matrix fluid with PMMA particles was performed. A suspension containing 0.85 of the maximum packing fraction of PMMA in HTPB was prepared. The mixing procedure was carried out for approximately 20 min to remove the air bubbles in the prepared suspension.

The procedure used during the characterization of rheological properties is very important. The same

TABLE I
R_a Values of the Metal Discs

R_a (μm)			
Cu discs	Brass discs	Stainless steel discs	Al discs
1.51	0.82	0.72	0.67
1.51	0.81	0.70	0.66
1.22	0.75		
1.21	0.75		
0.88	0.67		
0.86	0.66		
0.66	0.49		
0.63	0.49		

suspension preparation method was used for each experiment to get reproducible results.

R_a measurements and characterization of the construction materials of the disks used in the rheological characterization

During the experiments, aluminum, stainless steel, copper, brass, and glass were used as construction materials for the disks used in the rheological characterization. All of the disks were prepared within a certain R_a range.

Surface roughness evaluation is very important for many fundamental problems, including friction, contact deformation, heat and electric current conduction, tightness of contact joints, and positional accuracy. For this reason, surface roughness has been the subject of experimental and theoretical investigations for many decades. The real surface geometry is so complicated that a finite number of parameters cannot provide a full description. The arithmetic average height parameter (or R_a) is the most universally used roughness parameter for general quality control. This parameter is easy to define and easy to measure and gives a good general description of height variations. It is not sensitive to small changes in the profile. It is defined as the average absolute deviation of the roughness irregularities from the mean line over one sampling length. The mathematical definition and the digital implementation of R_a are as follows:[19]

$$R_a = \frac{1}{l}\int_0^l |y(x)|\, dx \qquad (2)$$

where l is the total length over which the measurements are made.

The R_a values of the disks were characterized by a roughmeter (Surtronic 3+, Rank Taylor Hobson Ltd., Leicester, UK). The R_a values of the disks were measured to be in the range 0.49–1.5 μm. This range is typical for surfaces produced by means of ordinary machine shop processing. The R_a values for each construction material are given in Table I. The R_a values of the disks were measured at five different places in the circumferential direction near the edge, and their average values are reported in Table I. To investigate the effect of construction material on viscosity and slip velocity, a set of disks were prepared by trial and error with R_a values of approximately 0.67 μm. The R_a values of the glass disks were not measured due to the possibility of damage to the glass disks with the diamond tip during the measurement process.

Some comparative adhesion measurements of the suspensions were also done with different construction materials. About 1 mL of PMMA and HTPB suspension with 85% of the maximum packing fraction was injected onto each glass or metal disk with similar roughness values and allowed to rest for 18 h. Then, the metal or glass disks were put in a vertical position for about 18 h to let the suspensions flow with gravity. Some amount of suspension was observed to flow out of the disk surface. The disks with the remaining amount of suspension were weighed, and the weight proportion of the remaining amount gave us an idea about the comparative adhesion energies of the suspensions and the discs. The results of this experiment are given in Table II. Each experiment, except for glass, was done with two sets of parallel disks, and the comparative percentage adhesion values were calculated with eq. (3):

$$\text{Comparative adhesion } (\%) = (w_{fs}/w_{0s}) \times 100 \qquad (3)$$

where w_{0s} is the initial weight of the suspension on the disk and w_{fs} is the final weight of the suspension on the disk. According to the results reported on Table II, aluminum disks had the highest adhesion energy in comparison to brass, copper, and stainless steel disks with similar R_a values. Glass had the lowest adhesion energy, possibly due to its nonmetallic properties and low R_a.

Experimental setup and procedure

In this study, the suspension samples were characterized by means of a Haake parallel disk rheometer

TABLE II
Comparative Adhesion Energy Experiment Results

Material	R_a (μm)	Comparative adhesion (wt %)
Al		
First run	0.67	92.4
Second run	0.66	93.9
Brass		
First run	0.66	91.6
Second run	0.67	85.3
Copper		
First run	0.66	88.7
Second run	0.63	85.9
Glass		
First run	—	40.3
Stainless steel		
First run	0.72	51.6
Second run	0.70	68.0

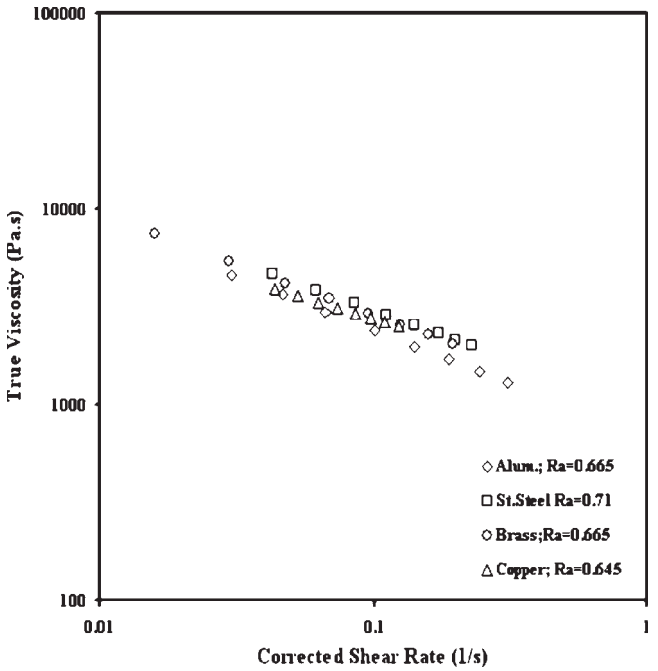

Figure 2 Effect of the construction material on the true viscosity.

(Haake GmbH, Bersdorff, Germany). The setup contained a Rotovisco RV20 with a measuring system, CV20, that was connected to a computer. Also, a water circulator was connected to the instrument to keep the temperature constant during the experiments. The Rotovisco RV20 controlled the electronic speed and the speed settings for the CV20 measuring system and provided a digital display to read the test results. The CV20 measuring system was comprised of a measuring unit and a sensor. The diameter of the used disks was 19.25 mm. All of the mixtures were characterized at a constant temperature of 25°C.

In the experiments, approximately 1 mL of the suspension was injected on the lower disk, and then, the upper disk was brought down, and the gap height was adjusted. The lower disk was rotated at a definite rotational speed by the direct-current drive motor, whereas the upper plate was held stationary. The resulting shear stress or torque was measured. The shear stress was measured in the steady-shear mode. The torsional flow behavior of the concentrated suspensions was characterized with various gap heights in the range 1–3 mm. Multiple gap heights were used to determine and incorporate slip at the wall corrections.[18,19] In each experiment, a fresh sample was injected, and preshearing of the sample was avoided.

RESULTS AND DISCUSSION

Highly concentrated suspensions exhibit time-dependent effects as well as yield, especially at high concentrations. Here, the suspension concentration that was chosen was smaller (54.9%) than the one used in ref. 16 (63%) to prevent such effects. The suspension did not exhibit yield or thixotropic/rheopectic effects. There was some stress overshoot, as observed for most polymer melts and suspensions. The steady-state values are reported. This also implies that there was no ordering or aggregation with time. Spherical fillers are in general less aggregating then nonspherical ones.

The volume fraction (85% of ϕ_m) and particle size (121.2 μm) of the particles were kept constant, and the true viscosity and slip velocity were determined with disks that were made from different construction material but that had approximately the same R_a (except for glass). The graphs of corrected viscosity versus corrected shear rate of the suspension obtained with different construction materials were obtained with procedures outlined in refs. 17, 18, and 20. As expected, the true viscosity of the suspensions shown in Figure 2 was observed to be independent of the construction materials.

On the other hand, the effect of construction material on slip velocity versus corrected shear stress is shown in Figure 3. The glass disk had the highest slip velocity at a constant shear stress value, and the aluminum disk had the lowest slip velocity at a constant shear stress value. Brass, copper, and stainless steel exhibited behaviors that were very close to each other and existed between the lines of aluminum and glass.

When the comparative adhesion energy experiments were correlated with the findings in Figure 3,

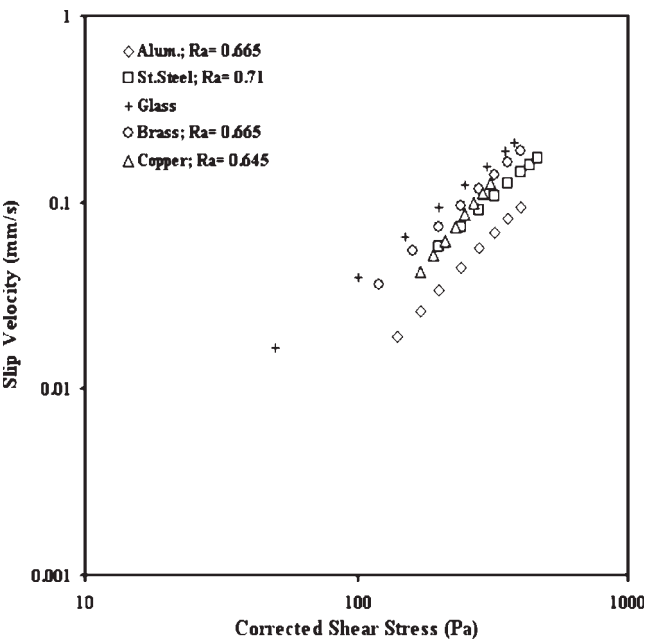

Figure 3 Effect of the construction material on the slip velocity.

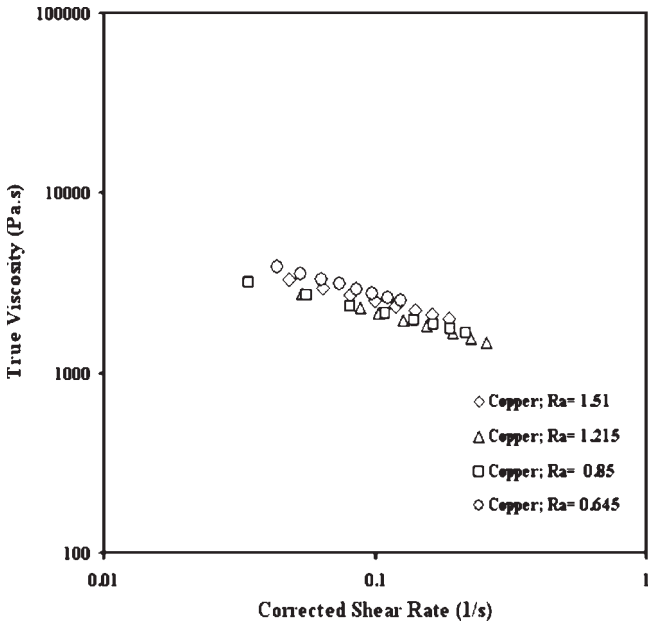

Figure 4 Effect of R_a on the true viscosity for copper.

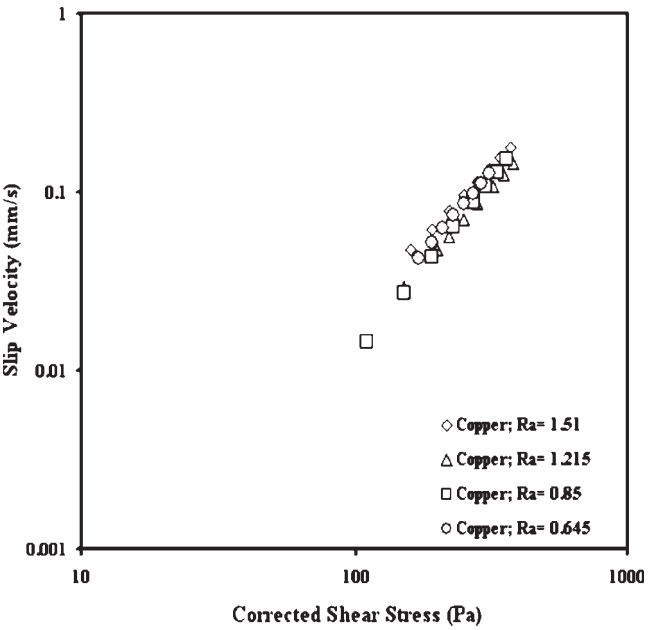

Figure 6 Effect of R_a on the slip velocity for copper.

glass had the lowest adhesion (40%) with the highest slip velocity. Moreover, aluminum had the highest adhesion (93%) with the lowest slip velocity. However, the adhesion energy results did not exhibit any significant trend between the slip velocity and the percentage adhesion for copper, brass, and stainless steel.

To observe the effect of R_a, experiments were done with copper and brass. The volume fraction (85% of ϕ_m) and particle size (121.2 μm) of the particles were kept constant. For copper, the R_a values were changed from 1.50 to 0.645 μm, whereas for brass, the R_a range was 0.815–0.49 μm.

The true viscosity of the suspensions did not change with R_a as expected. These results are shown in Figure 4 for copper and in Figure 5 for brass.

Another interesting observation was that the slip velocity of the suspensions did not significantly change with R_a at a constant shear stress. These results are shown in Figure 6 for copper and in Figure 7 for brass. The reason for this behavior is thought to be

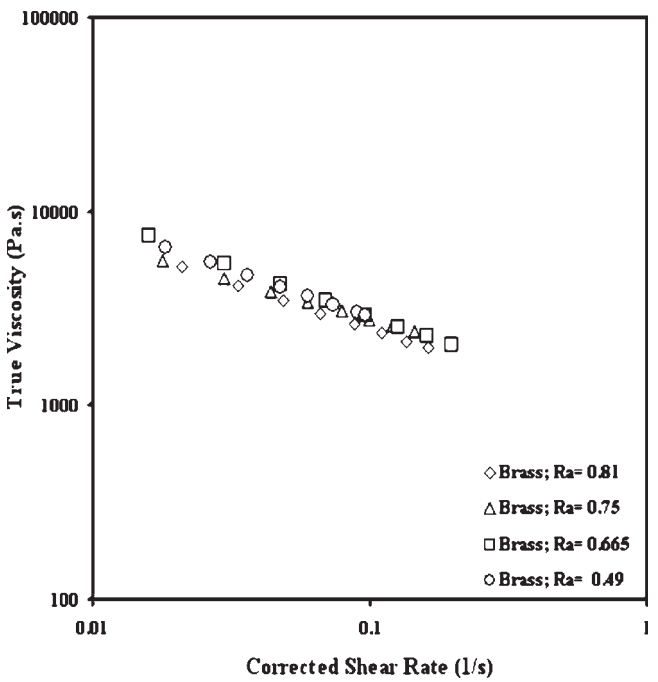

Figure 5 Effect of R_a on the true viscosity for brass.

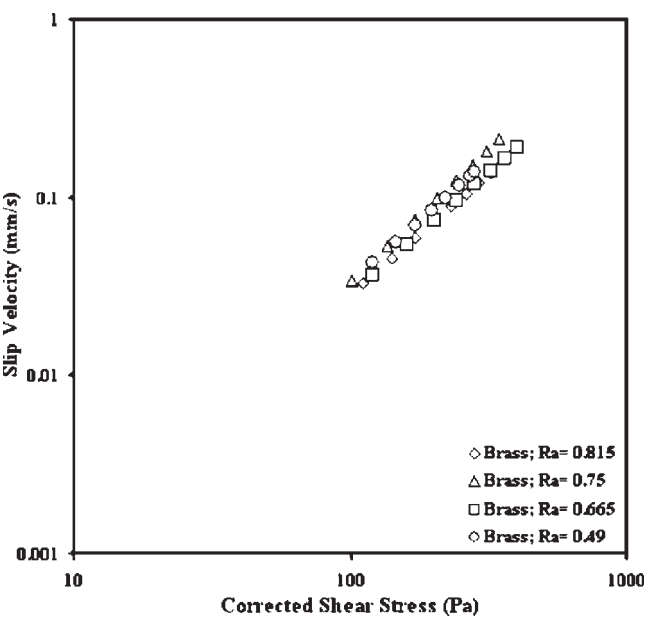

Figure 7 Effect of R_a on the slip velocity for brass.

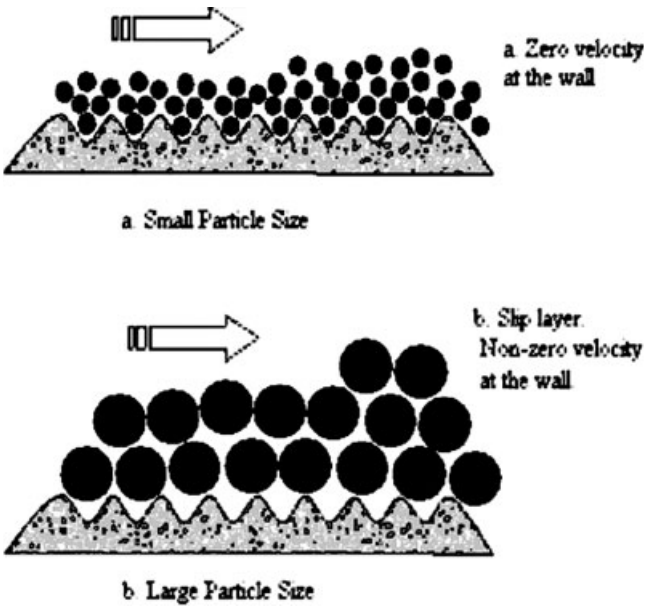

Figure 8 Schematic diagram for the effect of R_a-to-particle size ratio on the wall slip velocity.

the low R_a values (0.49–1.51 μm) in comparison to the average particle size (121.20 μm) studied. The particle size-to-R_a ratios studied were approximately 80–247. This phenomenon is explained by means of Figure 8. As shown in Figure 8, when small size particles flowed over a surface with roughness comparable to the average particle size, the roughness effects may have prevented slip, and the velocity of the particles near the wall was 0. On the other hand, if the sizes of the particles were much larger than R_a, the flow of particles was not affected by R_a, a slip layer formed, and the suspension exhibited slip at the wall.[17]

Aral and Kalyon[16] worked with a glass sphere/polybutadiene–acrylonitrile–acrylic acid matrix. The matrix was similar to the one used in this study (HTPB). However, these were the main differences:

- Their particle size was smaller. (85.4 vs 121.2 μm in this study).
- They studied particle size-to-R_a ratios of approximately 0.34 to 227.7 (with the assumption that their disks had a diameter of 12.5 mm). They observed slip roughly when the ratio was higher than 1 and no slip when this ratio was smaller than 1. Sample fracture was usually observed when slip did not occur. This ratio was between 80 and 247 in our study; thus, slip was observed for all of the cases studied.
- Their volume fraction was higher (63 vs 54.9% in this study). For this reason, in our case samples did not exhibit yield and time-dependent effects.

For the experimental conditions in this study, the slip velocities observed on mechanically processed surfaces could be independent of the R_a values because the particles were much larger than R_a. On the other hand, a dependency could be observed for the R_a values, which are comparable to the average particle sizes of the fillers.

CONCLUSIONS

The effects of R_a and construction material on the wall slip and viscosity of concentrated suspensions of PMMA particles in HTPB were investigated. The main conclusions of the study are as follows:

- The true viscosity of the suspension was independent of surface construction material and R_a as expected.
- As to the effect of surface construction material, glass had the highest slip velocity with the lowest adhesion (40%), and aluminum had the lowest slip velocity with the highest adhesion (93%).
- R_a did not have a significant effect on the wall slip and flow of suspensions for the particle size-to-R_a ratios studied here (80–247).

References

1. Vinogradov, G. V.; Froishteter, G. B.; Trilisky, K. K.; Smorodisnky, E. L. Rheol Acta 1975, 14, 765.
2. Vinogradov, G. V.; Froishteter, G. B.; Trilisky, K. K. Rheol Acta 1978, 17, 156.
3. Cohen, Y.; Metzner, A. B. Macromolecules 1982, 15, 1425.
4. Kraynik, A. M.; Schowalter, W. R. J Rheol 1981, 25, 95.
5. Jiang, T. Q.; Young, A. C.; Metzner, A. B. Rheol Acta 1986, 25, 397.
6. Ramamurthy, A. V. J Rheol 1986, 30, 337.
7. Chen, Y.; Kalyon, D. M.; Bayramli, E. J Appl Polym Sci 1993, 50, 1169.
8. Wang, S.; Drda, P. Macromolecules 1996, 29, 2627.
9. Wang, S.; Drda, P. A. Macromolecules 1996, 29, 4115.
10. Yang, X.; Ishida, H.; Wang, S. J Rheol 1998, 42, 63.
11. Yang, X.; Wang, S.; Halasa, A.; Ishida, H. Rheol Acta 1998, 37, 415.
12. Ghanta, V. G.; Riis, B. L.; Denn, M. M. J Rheol 1999, 43, 435.
13. Jabbarzadeh, A.; Atkinson, J. D.; Tanner, R. I. J Chem Phys 1999, 110, 2612.
14. Barone, J. R.; Wang, S. J. Non-Newtonian Fluid Mech 2000, 91, 31.
15. Kalyon, D. M.; Yaras, P.; Aral, B. K.; Yilmazer, U. J Rheol 1993, 37, 35.
16. Aral, B. K.; Kalyon, D. M. J. Rheol 1994, 38, 957.
17. Yoshimura, A. S.; Prudhomme, R. K. J Rheol 1988, 32, 53.
18. Yilmazer, U.; Kalyon, D. M. J Rheol 1989, 33, 1197.
19. Gadelmawla, E. S.; Koura, M. M.; Maksoud, T. M. A.; Elewa, I. M.; Soliman, H. H. J Mater Process Tech 2002, 123, 133.
20. Gulmus, S. A.; Yilmazer, U. J Appl Polym Sci 2005, 98, 439.